ORGANIC LETTERS

2012
Vol. 14, No. 4
1000–1003

Cruciforms' Polarized Emission Confirms Disjoint Molecular Orbitals and Excited States

Matthew N. Gard,[†] Anthony J. Zucchero,[‡] Gregory Kuzmanich,[†] Christian Oelsner,[§] Dirk Guldi,*[,§] Andreas Dreuw,*[,‖] Uwe H. F. Bunz,*[,⊥] and Miguel A. Garcia-Garibay*[,†]

Department of Chemistry, University of California, Los Angeles, California 90095-1559, United States, School of Chemistry and Biochemistry, Georgia Institute of Technology, Atlanta, Georgia 30332, United States, Department of Chemistry and Pharmacy & Interdisciplinary Center of Molecular Materials (ICMM), Friedrich-Alexander-Universität Erlangen-Nürnberg, Egerlandstr. 3, 91054 Erlangen, Germany, Interdisciplinary Center for Scientific Computing, Ruprecht-Karls Universität, Im Neuenheimer Feld 368, 69120 Heidelberg, Germany, and Organisch-Chemisches Institut, Ruprecht-Karls Universität, Im Neuenheimer Feld 270, 69120 Heidelberg, Germany

guldi@chemie.uni-erlangen.de; dreuw@uni-heidelberg.de; uwe.bunz@oci.uni-heidelberg.de; mgg@chem.ucla.edu

Received December 12, 2011

ABSTRACT

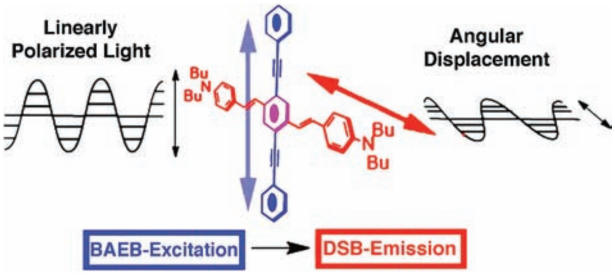

Steady-state and time-resolved polarized spectroscopy studies reveal that electronic excitation to the third excited state of 1,4-distyryl-2,5-bis(arylethynyl)benzene cruciforms results in fluorescence emission that is shifted an angle of ca. 60°. This result is consistent with quantum chemical calculations of the lowest electronic excited states and their transition dipole moments. The shift originates from the disjointed nature of the occupied molecular orbitals being localized on the different branches of the cruciforms.

Aromatic cross shaped chromophores, also known as cruciforms (XFs), have been the subject of numerous investigations for their remarkable electronic properties.[1] Among them, 1,4-distyryl-2,5-bis(arylethynyl)-benzene XFs **1**−**7**, sharing a common benzene core, are particularly interesting (Figure 1).[2] Molecular orbital calculations at the DFT/BHLYP level have shown that donor substituents on the distyryl branch (DSB, shown in red in Figure 2) and acceptor substituents on the bis(arylethynyl)benzene branch (BAEB, shown in blue) lead to spatial separation of the molecular orbitals,[3] such that

---

[†] University of California.
[‡] Georgia Institute of Technology.
[§] Friedrich-Alexander-Universität Erlangen-Nürnberg.
[‖] Interdisciplinary Center for Scientific Computing, Ruprecht-Karls Universität.
[⊥] Organisch-Chemisches Institut, Ruprecht-Karls Universität.

(1) (a) Marsden, J. A.; Miller, J. J.; Shirtcliff, L. D.; Haley, M. M. *J. Am. Chem. Soc.* **2005**, *127*, 2464–2476. (b) Christian-Pandya, H. K.; Niazimbetova, Z. I.; Beyer, F. L.; Galvin, M. E. *Chem. Mater.* **2007**, *19*, 993–1001. (c) Kang, H.; Evmenenko, G.; Dutta, P.; Clays, K.; Song, K.; Marks, T. J. *J. Am. Chem. Soc.* **2006**, *128*, 6194–6205. (d) Davey, E. A.; Zucchero, A. J.; Trapp, O.; Bunz, U. H. F. *J. Am. Chem. Soc.* **2011**, *133*, 7716–7718. (e) Zen, A.; Bilge, A.; Galbrecht, F.; Alle, R.; Meerholz, K.; Grenzer, J.; Neher, D.; Scherf, U.; Farrell, T. *J. Am. Chem. Soc.* **2006**, *128*, 3914–3915.

(2) Zucchero, A. J.; McGrier, P. L.; Bunz, U. H. F. *Acc. Chem. Res.* **2010**, *43*, 397–408.

(3) (a) Wilson, J. N.; Windscheif, P. M.; Evans, U.; Myrick, M. L.; Bunz, U. H. F. *Macromolecules* **2002**, *35*, 8681–8683. (b) Wilson, J. N.; Josowicz, M.; Wang, Y.; Bunz, U. H. F. *Chem. Commun.* **2003**, 2962–2963. (c) Wilson, J. N.; Hardcastle, K. I.; Josowicz, M.; Bunz, U. H. F. *Tetrahedron* **2004**, *60*, 7157–7167.

10.1021/ol203321m

certain orbitals reside only along the DSB moiety while others are mainly localized in the BAEB branch (Figure 1).

XFs provide control over conjugation through changes in planarization in ordering media.[4–6] It has been suggested that suitably derivatized cruciforms may be used as molecular switches by engineering the response of one branch to the presence of external fields.[7,8] Due to disjointed frontier molecular orbitals, oxidation and reduction in a cruciform will occur in different branches,[3,9,10] and they will have transition dipole moments that are 60° apart. Intriguing features of this electronic arrangement are the possibility for directional control of electron and hole transport and its use as a molecular tool for the photonic manipulation of polarized light.

The localized occupied molecular orbitals on DSB and BAEB branches suggest that corresponding excited states involving electronic transitions from the HOMO or HOMO-2 to the LUMO should possess strongly rotated transition dipole moments. One can recognize that, according to this model, polarized excitation into the HOMO-2→LUMO excited state should result in emission from the HOMO→LUMO state with light rotated by an angle of 60°, providing a means to shift the frequency and polarization angle of incident light when the frame of reference of the molecule is maintained constant. Here we confirm these expectations with steady-state and time-resolved polarization studies carried out with XFs **1**–**7** (Figure 2), which according to our quantum chemical calculations possess two strongly allowed S_4 and S_1 states corresponding to the HOMO-2→LUMO and HOMO→LUMO transitions.

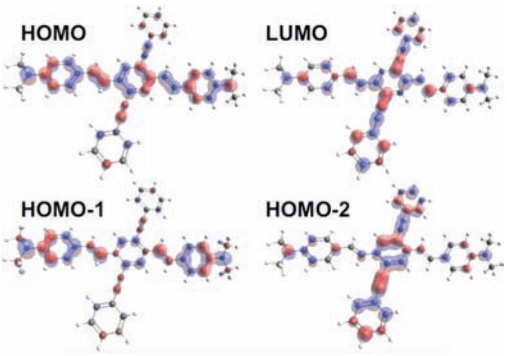

Figure 1. DFT/BHLYP/cc-pVDZ frontier molecular orbitals of cruciform **1** illustrating the HOMOs and the LUMO largely localized in the DSB and BAEB branches, respectively.

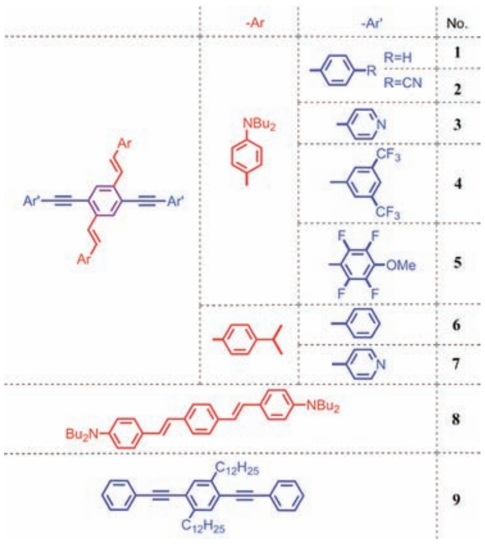

Figure 2. Structure key for compounds **1**–**9**.

XFs **1**–**5** have electron-donating dibutylamino substituents attached at the 4′-DSB positions. The aromatic substituents on the BAEB branches of **1**–**5** are phenyl (**1**), *p*-cyanophenyl (**2**), 4-pyridyl (**3**), 3,5-bis(trifluoromethyl)-phenyl (**4**), and 2,3,5,6-tetrafluoro-4-methoxyphenyl (**5**). Compounds **6** and **7** have isopropyl substituents at the 4′-positions of the DSB branch with phenyl and pyridyl groups, respectively, on the BAEB segment. Compounds **8** and **9** represent model DSB and BAEB chromophores to characterize the properties of the two branches.

The extent by which the two XF branches electronically perturb each other can be estimated by comparing their UV absorption spectra with those of the linear model chromophores. The experimental UV absorption spectra of **8** and **9** in methylcyclohexane are shown in Figure 3 while the spectrum of cruciform **1** in the same solvent is plotted in a solid black line. The spectrum of the linear dibutylamino-substituted DSB **8**, shown in red in Figure 3, has a lowest energy absorption band between 350 and 450 nm with a λ_{max} = 402 nm and two shoulders at 423 and 350 nm, assigned to the vibrational progession of the C═C stretch mode.[11] The spectrum of **1** is red-shifted by *ca.* 25 nm, and it shows a change in the Franck–Condon factors of the vibronic features. Hypsochromically shifted and with a weaker S_0–S_1 transition, the linear BAEB **9** has a λ_{max} = 325 nm and has a similar position in the spectrum as the corresponding band in XF **1**.[12] Calculations of the excited states employing time-dependent density functional theory (TDDFT) with the BHLYP exchange-correlation functional and the standard cc-pVDZ basis set reveal both states as $\pi\pi^*$ excitations from the HOMO

---

(4) (a) Levitus, M.; Schmieder, K.; Ricks, H.; Schimizu, K. D.; Bunz, U. H. F.; Garcia-Garibay, M. A. *J. Am. Chem. Soc.* **2001**, *123*, 4259–4265. (b) Schmieder, K.; Levitus, M.; Dang, H.; Garcia-Garibay, M. A. *J. Phys. Chem. A* **2002**, *105*, 1551–1556.

(5) Terphenyl-bis(phenyl)oxazole cruciforms have been used to control the deposition of molecules on electrode surfaces: Klare, J. E.; Tulevski, G. S.; Sugo, K.; Picciotto, A.; White, K. A.; Nuckolls, C. *J. Am. Chem. Soc.* **2003**, *125*, 6030–6031.

(6) Nakayama, H.; Imura, S. *J. Phys. Chem. A* **2011**, *115*, 8960.

(7) Blaszczyk, A.; Fischer, F.; von Hänisch, C.; Mayor, M. *Eur. J. Org. Chem.* **2007**, 2630–2642.

(8) Grunder, S.; Huber, R.; Horhoiu, V.; Gonzalez, M. T.; Schönenberger, C.; Calame, M.; Mayor, M. *J. Org. Chem.* **2007**, *72*, 8337–8344.

(9) (a) Jennum, K.; Nielsen, M. B. *Chem. Lett.* **2011**, *40*, 662667.

(10) Zhou, N.; Wang, L.; Thompson, D. W.; Zhao, Y. *Tetrahedron Lett.* **2007**, *48*, 3563.

(11) Bush, T. E.; Scott, G. W. *J. Phys. Chem.* **1981**, *85*, 144.

(12) Brombosz, S. M.; Zucchero, A. J.; McGrier, P. L.; Bunz, U. H. F. *J. Org. Chem.* **2009**, *74*, 8909–8913.

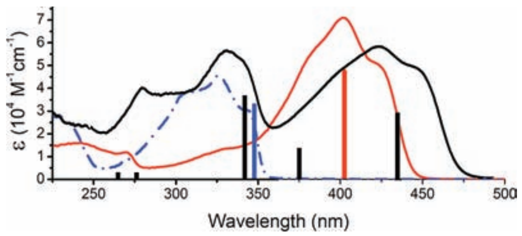

Figure 3. Absorption spectra of DSB **8** (solid red), BAEB **9** (dot-line blue), and **1** (solid black) in methylcyclohexane. The stick spectra in the corresponding colors correspond to the vertical excited states computed at the TDDFT/BHLYP/cc-pVDZ level consistently shifted by −0.2 eV to correct for missing solvent effects and easy comparison with experiment.

to the LUMO of the respective molecules.[13] The vertical excitation energies of these strongly allowed S_1 states have values of 3.27 and 3.76 eV at this level of theory, exhibiting a systematic error of +0.2 eV. In Figure 3, the corresponding stick spectra shifted by −0.2 eV are compared with the experimental ones.

The absorption spectrum of cruciform **1** has analogous absorption bands between 255 and 485 nm and is similar to the spectrum obtained by summation of **8** and **9**. The lowest energy DSB-related transition of the XF is red-shifted by ca. 22 nm compared to that of **8**. The higher energy band is not significantly affected (Figure 3). Indeed, TDDFT/BHLYP calculations reveal the first absorption band to consist of two excited states, one a very strongly allowed S_1 and one a weaker S_2 state with calculated absorption wavelengths of 429 and 372 nm (adjusted for an intrinsic error of 0.2 eV, Figure 3). While S_1 can best be described as an excitation from the HOMO to the LUMO, S_2 corresponds to a HOMO-1 to LUMO transition (Figure 1). Both, HOMO and HOMO-1 are located on the DSB branch, while the LUMO is delocalized with larger contributions on the BAEB branch. The second broad peak of the absorption spectrum is due to the strongly allowed S_4 state with a computed absorption wavelength of 340 nm. This state corresponds to a single electron transition from the HOMO-2 into the LUMO and is most closely related to the S_1 of **9**. The S_3 state of **1** is one-photon forbidden and thus not visible in the spectrum.

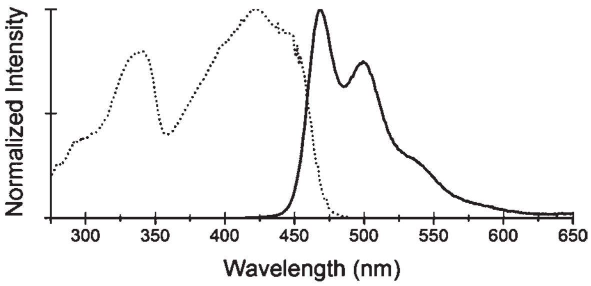

Figure 4. Excitation (dotted line) and emission spectra (solid line) of cruciform **1** in methylcyclohexane.

The emission spectrum of **1** is quite similar to that of DSB **8** but red-shifted by ca. 50 nm (Figure 4). Similar observations regarding absorption, excitation, and emission spectra were made with **2**–**5**, all which have been previously published.[14] The fluorescence quantum yields (Φ_{Fl}) and lifetimes (τ_{Fl}) for **1**–**9** are included in Table 1. The photophysical properties determined for this study in CH_2Cl_2 are in good agreement with those previously reported in $CHCl_3$.[14] The angular shift in linear polarization that occurs upon light absorption and emission, defined by the angle β, was determined as a function of excitation wavelength for XFs **1**–**7** by measuring the steady-state fluorescence anisotropy, r_{SS}, in viscous mineral oil, and the fundamental anisotropy, r_0, in dichloromethane solution. Both measurements provided similar results consistent with the cartoon model shown in the table of contents graphic. The steady-state fluorescence anisotropy, r_{SS}, and the fundamental anisotropy, r_0, are defined in eqs 1 and 2, respectively.[15,16]

$$r_{SS} = (I_{hh} - GI_{hv})/(I_{hh} + 2GI_{hv}) \tag{1}$$

$$r_0 = \frac{2}{5}\left(\frac{3\cos^2\beta - 1}{2}\right) \tag{2}$$

The r_{SS} values are determined by analyzing the intensity (I) of the steady-state emission using polarizers in the excitation and emission beams that are parallel (hh: both horizontal) and perpendicular (hv: one horizontal and one perpendicular). The correction factor, G, is related to the experimental setup. The fundamental anisotropy r_0 is obtained by measuring the time-resolved fluorescence anisotropy and extrapolating its value to $t = 0$. The time-resolved fluorescence anisotropy [$r_{SS}(t)$] is determined using eq 1 with I_{hh} and I_{hv} measured as a function of time during the lifetime of the excited state. As indicated by eq 2, the value of r_0 depends on the angle β that exists between the transition dipoles moments for absorption and emission.

For single photon processes, the fundamental anisotropy in a sample with molecules oriented randomly in solution has a maximum value of $r_0 = 0.4$ if the transition dipoles for absorption and emission are collinear ($\beta = 0°$).[17] A minimum with $r_0 = -0.2$ occurs when the transition

---

(13) (a) Dreuw, A.; Head-Gordon, M. *Chem. Rev.* **2005**, *105*, 4009–4037. (b) Becke, A. D. *J. Chem. Phys.* **1993**, *98*, 1372–1378.

(14) Zucchero, A. J.; Wilson, J. N.; Bunz, U. H. F. *J. Am. Chem. Soc.* **2006**, *128*, 11872–11881.

(15) Michl, J.; Thulstrup, E. W. *Spectroscopy with Polarized Light: Solute Alignment by Photoselection. Liquid Crystals, Polymers and Membranes*; VCH Publishers: New York, 1995. (b) Thulstrup, E. W.; Michl, J. *J. Am. Chem. Soc.* **1982**, *104*, 5594.

(16) Lakowicz, J. R. In *Principles of Fluorescence Spectroscopy*; Plennum Press: New York, 1993.

(17) It is not uncommon for the experimental limiting anisotropy to be different than 0.4. For example, see: Valeur, B. *Molecular Fluorescence. Principles and Applications*; Wiley-VCH: Weinheim, 2002.

Table 1. Fluorescence and Anisotropy Data for Cruciforms **1**–**7** and Compounds **8** and **9**

compd	τ_{Fl} (ns) hex	τ_{Fl} (ns)[a] CH_2Cl_2	r_{SS} min oil	r_0[b] $CHCl_3$	Φ_{Fl} CH_2Cl_2
1	1.08	1.16	0.32	0.25	0.31
2	2.03	3.32	0.20	0.23	0.05
3	1.75	2.34	0.28	0.25	0.11
4	3.99	4.37	0.23	0.27	0.09
5	2.20	2.71	0.17	0.18	0.15
6	2.39	2.18	0.12	0.24	–
7	3.48	3.92	0.28	0.22	0.31
8	0.90	1.02	0.34	0.32	0.88
9	0.68	0.74	–	0.21	–

[a] In excellent agreement with values in $CHCl_3$ reported in ref 14. [b] Measured by excitation at 403 nm ($S_0 \longrightarrow > S_1$) and detecting at 480 nm ($S_0 \longrightarrow > S_1$).

dipoles are at $\beta = 90°$. As expected, the anisotropy goes to zero at the magic angle, $\beta = 54.7$. The fundamental anisotropy is equal to the steady-state anisotropy, r_{ss}, only when there are no depolarization pathways, such as rotational diffusion or energy transfer (such as FRET). While energy transfer should be negligible for isolated chromophores in dilute solution, molecular rotation can be slowed down significantly by using a very viscous solvent. For that reason, compounds **1**–**9** were analyzed in dilute solutions in heavy mineral oil (kinematic viscosity larger than 34.5 cSt at 40 °C). If there is no rotation within the 0.7–4.4 ns lifetime of the cruciform excited state, the steady-state anisotropy, r_{ss}, should be identical to the fundamental anisotropy r_0, which can be used to calculate the angular displacement of the transition dipole moments for excitation and emission, β, using eq 2.

A plot of r_{SS} vs excitation wavelength for cruciforms **1**–**7** detected at their emission maximum showed values that range from $r_{SS} = -0.05$ to $r_{SS} = 0.35$. From the anisotropy results one can identify three regions corresponding to what appears to be a mixed transition band between 250 and 275 nm with $r_{SS} = 0.1$, a band corresponding to the absorption by the BAEB branch with a negative anisotropy value $r_{SS} = -0.05$, and band associated with DSB absorption with a large and positive anisotropy of 0.35, which is close to the theoretical maximum of 0.4 (Supporting Information).

To confirm that there is no molecular rotation in mineral oil during the lifetime of their excited states we carried out a series of fluorescence anisotropy decay measurements with all cruciforms. The results of measurements carried out by excitation at 403 nm ($S_0 \longrightarrow > S_1$) and detection at 480 nm ($S_0 \longrightarrow > S_1$) are included in Table 1 next to the corresponding steady-state values in mineral oil. Having confirmed that excited state lifetimes in $CHCl_3$ and in hydrocarbons at a chosen wavelength are very similar, we assume that all r_{SS} values in mineral oil represent the desired r_0 values at all wavelengths. Then we used eq 2 to calculate the effective polarization shift angle as a function of wavelength.

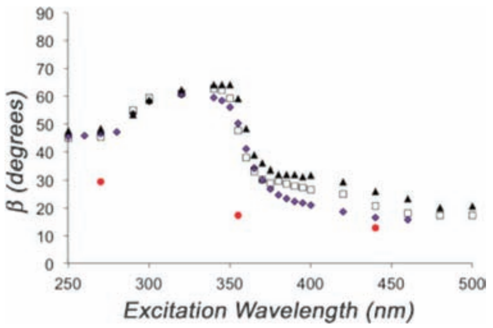

Figure 5. Plot of excitation wavelength vs β for cruciforms **1** (diamonds, $\lambda_{em} = 480$ nm), **3** (hollow squares, $\lambda_{em} = 520$ nm), **4** (triangles, $\lambda_{em} = 520$ nm) and compound **8** (red circles, $\lambda_{em} = 480$ nm). The value of β in degrees represents the angular displacement between the excitation and emission transition dipole moments.

The results in Figure 5 include data points (red circles) for the model DSB **8** and data points for cruciforms **1**, **3**, and **4** with fluorescence anisotropy detected at different emission wavelengths. One can see that the polarization shift angle increases with the excitation wavelength beyond $\lambda_{ex} = 275$ nm, reaching a maximum of ca. 67° between $\lambda_{ex} = 300$ and 350 nm. At longer wavelengths of $\lambda_{ex} = 350$–400 nm a shift angle of ca. 25° is observed. While the first plateau corresponds to the region where absorption into the S_4 is nearly pure, beyond 350 nm excitation into S_2 takes place. Indeed, the observed shift angles are in excellent agreement with the calculated angles between the transition dipole moments of the absorbing and emitting states at the TDDFT/BHLYP level. The computed shift angle between S_2 and S_1 amounts to 24.3°, and that between S_4 and S_1 to 76.1°.

In conclusion, steady-state and time-resolved fluorescence anisotropy measurements together with quantum chemical calculations demonstrate that the two branches of DSB-BAEB XFs significantly retain individual electronic character during light absorption and emission events. This observation is consistent with the disjointed nature of their occupied molecular orbitals. It was confirmed that internal conversion following excitation into the BAEB-related S_4 state occurs by a change in polarization angle of ca. 67°, disclosing a property that could be useful if one considers applications in the field of molecular photonics.

Acknowledgment. We thank NSF Grants DMR1101934 and DGE-0654431 (IGERT: Materials Creation Training Program).

Supporting Information Available. Experimental details of sample preparation and fluorescence anisotropy measurements. Computational details of method evaluation and tests. This material is available free of charge via the Internet at http://pubs.acs.org.

The authors declare no competing financial interest.